ELSEVIER

Applied Catalysis B: Environmental 29 (2001) 217–229

APPLIED CATALYSIS B: ENVIRONMENTAL

www.elsevier.com/locate/apcatb

Catalytic combustion of methane on Co/MgO: characterisation of active cobalt sites

M.A. Ulla [a], R. Spretz [a], E. Lombardo [a], W. Daniell [b], H. Knözinger [b,*]

[a] *Instituto de Investigaciones en Catálisis y Petroquímica, INCAPE (FIQ, UNL-CONICET), Santiago del Estero 2829, C.P. 3000, Santa Fe, Argentina*

[b] *Department Chemie, Physikalische Chemie, Ludwig Maximilians Universität, Butenandtstr. 5-13, Haus E, D-81377 München, Germany*

Received 12 March 2000; received in revised form 6 July 2000; accepted 6 July 2000

Abstract

A series of Co/MgO catalysts with 3–12 wt.% Co were prepared by impregnation and calcined at 1073 K for 10 h. The catalytic behaviour of these samples toward CH_4 combustion was found to increase with cobalt loading, though a plateau was reached at ca. 9 wt.% Co content. Bulk characterisation was carried out using XRD, TPR and Raman spectroscopy, and showed that the solids were made up of a CoO–MgO solid solution and a MgO phase. A detailed examination of their surfaces was achieved through FTIR spectroscopy of adsorbed CO probe molecules, which indicated that at low cobalt loadings only a small proportion of the Co going into the solid solution was present on exposed faces as either Co^{2+} oxo-species or pentacoordinated Co^{2+}. However, as the cobalt content of the samples increased, a larger amount was exposed on the surface. This effect levelled off at 9 wt.% Co, after which the increase in exposed Co^{2+} sites was countered by the masking effect of islands of MgO. In addition, at high cobalt loadings (9 and 12 wt.%) Co formed small clusters which showed bulk CoO-like behaviour. Consequently, the benefit of having surface Co^{2+} species was balanced by the clustering effect of these species and the presence of MgO islands, negating their contribution to the overall catalytic activity of the samples.

Keywords: Cobalt; Magnesium oxide; CoO–MgO solid solution; Methane combustion; CO adsorption; FTIR spectroscopy

1. Introduction

Catalytic combustion is a strategy employed to bring about the total oxidation of fuels, thereby making the combustion process more controllable and energy efficient, and reducing the emission of pollutants [1]. One vitally important application of this process is to be found in power stations where the catalytic combustion of natural gas (methane) at high temperature is used to drive gas turbines. In such cases, the catalysts employed are exposed to severe conditions, under which it is necessary to strike a balance between the activity of the catalyst and properties such as thermal and mechanical stability.

Co_3O_4 has proved to be a good catalyst for methane combustion [2], but unfortunately, undergoes severe sintering from 800 K upwards which drastically decreases its catalytic activity. This sintering process can be avoided, or at least deterred, through the use of a support which leads to the stabilisation of cobalt ions [3]. Magnesium oxide (MgO) has previously been reported as being a suitable support for methane combustion at high temperature, displaying a high melting point and thermal stability, and being able to main-

* Corresponding author. Fax: +49-89-2180-7605.
E-mail address: helmut.knoezinger@cup.uni-muenchen.de (H. Knözinger).

0926-3373/01/$ – see front matter
PII: S0926-3373(00)00204-6

tain a relatively high surface area ($25\,m^2\,g^{-1}$) under extreme reaction conditions [4]. This support also displays moderate activity towards hydrocarbon oxidation [5] which can be noticeably enhanced on addition of cobalt [6]. It is known that formation of solid solutions between CoO and MgO can occur over a wide concentration range, mainly due to the similar size of Co^{2+} and Mg^{2+} ions [7], in which the Co^{2+} ions occupy octahedral positions in the MgO lattice [8,9]. Therefore, for catalytic activity towards oxidation reactions to be retained in Co/MgO systems, it would appear that the support must also somehow stabilise surface cobalt ions.

In this work, a series of Co/MgO samples with Co loading up to 12 wt.% were prepared. The catalytic behaviour of these solids towards methane combustion was tested and the bulk material characterised through use of powder X-ray diffraction (XRD) and Raman spectroscopy. However, in order to understand more fully to the catalytic process and the influence of Co loading upon the catalytic activity, a detailed examination of the catalyst surface was required. This was achieved by Fourier transform infrared (FTIR) spectroscopy of adsorbed carbon monoxide (CO) probe molecules. The selection of CO as a probe for surface Lewis acid sites (LAS) is well-documented [10,11], and has been reported in previous studies investigating CoO–MgO solid solutions [12–15]. The aim of this work, therefore, was to investigate the distribution of surface Co sites in samples with varying Co loading, and relate their presence to the observed catalytic activity.

2. Experimental

2.1. Sample preparation

Co/MgO samples containing 3, 6, 9 and 12 wt.% Co were prepared from a MgO (Merck, p.a.) suspension in water, to which an aqueous $Co(NO_3)_2$ (Merck, p.a.) solution was added. The varying Co loadings were achieved through alteration of the molality of the $Co(NO_3)_2$ solution. The resulting mixture was evaporated under vigorous stirring until dryness. The solid thus obtained was heated overnight at 390 K, then calcined in air at 1070 K for 10 h. The BET surface areas of the Co/MgO samples were found to slightly decrease with Co loading. The values of 29.3, 31.7, 24.4 and $22.4\,m^2\,g^{-1}$ were recorded for the 3, 6, 9 and 12 wt.% Co samples, respectively (cf. $30.0\,m^2\,g^{-1}$ for MgO).

With the intention of producing samples for reference purposes consisting of a CoO–MgO solid solution (Co/Mg = 1.0), two samples were prepared by mixing two (0.5 M) solutions of $Co(NO_3)_2$ and $Mg(CH_3COO)_2$ (Merck, p.a.), to which citric acid dissolved in a minimum amount of water was added. The resulting solution was dried at 390 K overnight, and the porous solid thus obtained ground and then heated in air at 1070 and 1220 K for 10 h. These samples are designated CoO–MgO (1070) and CoO–MgO (1220), respectively.

A single Co/SiO_2 sample (2 wt.% Co) was prepared by impregnation of SiO_2 (Aldrich p.a.) with an aqueous solution of $Co(NO_3)_2$ via the incipient wetness method. The resulting gel was calcined in air at 1020 K for 2 h.

2.2. Catalyst testing

Catalytic combustion of methane was carried out using a 4 mm diameter quartz reactor in a fixed-bed continuous-flow system, with the catalyst fixed centrally in the reactor between two quartz wool plugs. Samples (0.05 g) with particle size between 177–250 μm were used for each test. A gas mixture composition of CH_4, 2 vol.%; O_2, 8 vol.%; N_2, balance was employed, with a space velocity of $480{,}000\,h^{-1}$, high enough to minimise any reaction induced thermal effects. Reactions were carried out at various temperatures within the range 820–895 K, and temperatures were measured using a thermocouple attached to the reactor wall. To achieve steady state, the reactor was kept at each temperature for 30 min before catalytic conversion measurements. The products were analysed by an on-line gas chromatograph, using a Porapak Q column for separation connected to a thermal conductivity detector (TCD). The kinetic studies were performed using conversion data attained with the reactor operating under differential conditions. Catalyst stability was checked by keeping each catalyst on stream for 24 h at the maximum reaction temperature. The absence of diffusion limitations were checked applying the Weisz criterion assuming the most unfavourable reaction conditions used.

2.3. Bulk characterisation

Crystalline phases within the prepared samples were identified by powder X-ray diffraction (XRD) analysis using a Shimadzu XD-D1 diffractometer, equipped with a Cu Kα radiation source and using a scanning rate of $1^\circ\,min^{-1}$ The Shimadzu XD-D1 analysis software package was used for the calculation of lattice parameters and phase identification.

TPR (temperature programmed reduction) experiments were carried out in an Okhura TS-2002 instrument. Typically, 50 mg of solid were pretreated in flowing O_2 at 870 K for 2 h and subsequently cooled in an Ar atmosphere to 320 K over a period of 1 h. The TPR was performed using 2 vol.% hydrogen in argon (flow rate: $40\,cm^3\,min^{-1}$) with a heating rate of $10\,K\,min^{-1}$ up to 1170 K, and a TCD detector.

Raman spectra were recorded under ambient conditions on a JASCO TRS-6000SZ-P Multichannel Laser Raman spectrometer. The excitation source was the 514.5 nm line of a Spectra 9000 Photometrics Ar ion laser, with laser power (measured at the sample) set at 30–40 mW.

2.4. Surface characterisation

FTIR spectroscopic studies were carried out on a Bruker IFS 66 spectrometer (MCT detector) at a resolution of $2\,cm^{-1}$ over 128 scans. Adsorption of CO was made at 85 K and achieved using a purpose-built, in situ IR cell (CaF_2 windows) connected to a vacuum/gas dosing system, and attached to a quartz reactor in which pretreatment was carried out. All samples were treated in flowing oxygen at 870 K for 2 h, and then under vacuum at the same temperature for 30 min, before cooling to 85 K under vacuum. Reduced samples underwent an additional pretreatment step in flowing H_2 at 870 K for 1 h, before subsequent evacuation and cooling. The reduction temperature was chosen to lie within the temperature range in which the catalytic combustion of methane was carried out. Peak intensities for the two peaks at 2148 and $2157\,cm^{-1}$ were obtained by deconvolution of the band envelope using the non-linear curve fit feature of the Origin software package, and integrating under the peak area.

3. Results

3.1. Catalytic activity

Fig. 1 shows the initial reaction rate for methane oxidation over the four Co/MgO (3–12 wt.% Co) samples and the MgO support at different temperatures (820–895 K). The initial reaction rate increases for each Co/MgO sample with reaction temperature. It is also clear that the addition of Co is beneficial for this reaction, seeing as the MgO support is totally inactive under the conditions studied. Note, that the reaction rate levels off at cobalt content ca. 9 wt.%. This is prominently displayed in the upper trace taken at 895 K.

3.2. Bulk characterisation

3.2.1. XRD analysis

XRD analysis was carried out on all four Co/MgO samples and three related samples (for comparison) in order to observe (a) segregation and sintering of a Co_3O_4 phase, and (b) formation of a CoO–MgO solid solution. The three reference samples were Co(2 wt.%)/SiO_2 and the intended CoO–MgO solid solution, calcined at both 1070 and 1220 K.

The diffraction pattern of Co/SiO_2 after calcination at 1020 K revealed the presence of Co_3O_4. In the case of CoO–MgO calcined at 1220 K, five peaks were

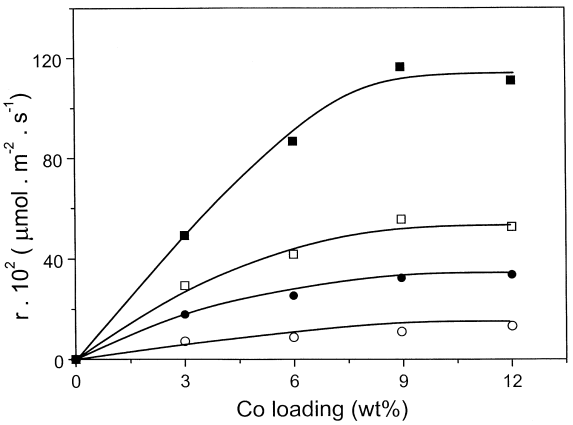

Fig. 1. Methane combustion rate as a function of Co loading at different reaction temperatures. Reaction conditions: CH_4 2 vol.%; O_2 8 vol.% and N_2 balance. Space velocity: $480{,}000\,h^{-1}$. Symbols: (○) 820 K, (●) 845 K, (□) 870 K, (■) 895 K.

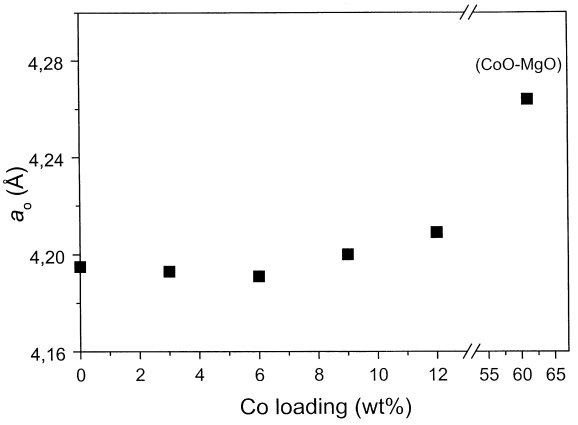

Fig. 2. Variation in lattice parameter a_o with Co loading (wt.%). Note: 61 wt.% Co corresponds to a homogeneous CoO–MgO solid solution calcined at 1220 K.

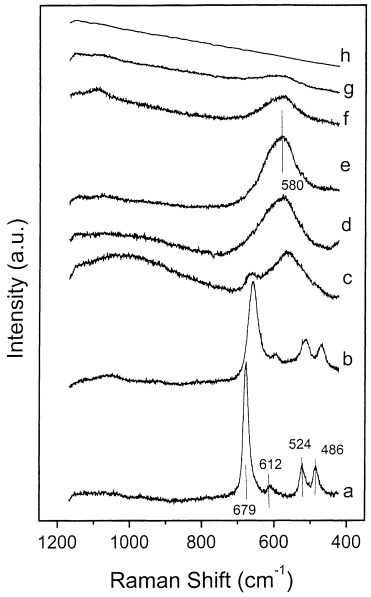

Fig. 3. Raman spectra of (a) Co(2 wt.%)/SiO_2 calcined at 1020 K; (b) CoO–MgO calcined at 1070 K; (c) CoO–MgO calcined at 1220 K; (d) Co(12 wt.%)/MgO; (e) Co(9 wt.%)/MgO; (f) Co(6 wt.%)/MgO; (g) Co(3 wt.%)/MgO; (h) MgO.

observed. In order to interpret these reflections, it is necessary to take into account that in homogeneous solid solution of CoO–MgO, Co^{2+} occupies Mg^{2+} sites in the MgO lattice without any reconstruction. Hence, MgO and CoO–MgO have reflections at near identical 2θ positions, but some differences in the lattice parameters are observed. MgO has a cubic structure and substitution of Co in the MgO structure increases the value of the a_o lattice parameter. In Fig. 2 the value of a_o for CoO–MgO compared with pure MgO can be seen. Hence, XRD confirms that the CoO–MgO sample calcined at 1220 K forms a homogeneous solid solution. For CoO–MgO calcined at 1070 K, the three main XRD peaks of Co_3O_4 are identified ($2\theta = 31.2$, 36.7 and 64.9°) along with five extra signals associated with the solid solution.

The XRD patterns of Co(x)/MgO ($x = 3$, 6, 9 and 12 wt.%) show the same five peaks characteristic of MgO and CoO–MgO solid solutions. The a_o parameters are close to that of the support for low Co loading suggesting that the main phase is MgO on Co(3 wt.%)/MgO and Co(6 wt.%)/MgO (Fig. 2). However, some distortion in this parameter is observed for high Co contents ($x = 9, 12$) indicating that a bulk solid solution coexists with MgO.

3.2.2. TPR

The amount of reducible species in Co/MgO samples is very low. According to TPR results, the H_2 consumption value of Co(9 wt.%)/MgO between 470–870 K is ca. 0.007 H_2/Co. By comparison, unsupported Co_3O_4 has reduction peaks around 620 K and a value of H_2/Co = 1.33. The same result is obtained for Co/SiO_2, whereas for the MgO support alone the H_2 consumption is negligible. This indicates that most of the Co in Co/MgO is present in the form of non-reducible oxides.

3.2.3. Raman spectroscopy

The Raman spectrum of Co/SiO_2 (Fig. 3a) shows the four characteristic vibrational signals of Co_3O_4 [16]: a sharp, intense signal at 679 cm^{-1}, a weak band at 612 cm^{-1} and two bands at Fig. 3b) also presents the Co_3O_4 bands, although a slight shift to lower frequencies is 524 and 483 cm^{-1}. The Raman spectrum of the CoO–MgO (1070) sample (Fig. 3b) also presents the Co_3O_4 bands, although a slight shift to lower frequencies is observed for all of these signals. This shift in band positions can be explained by different metal-support interactions. It is worth noting that there are no vibrational signals for MgO in this frequency range (Fig. 3g). When CoO–MgO is treated at high temperature (1220 K), a solid solu-

tion forms, radically changing the Raman spectrum (Fig. 3c), and giving a broad, moderately intense signal at 580 cm^{-1} and a shoulder at 665 cm^{-1}. This shoulder is close to the most intense peak of Co_3O_4 (comparing the spectrum in Fig. 3c with Fig. 3a and b) suggesting the presence of this species even though it is not detected through XRD. The broad band around 580 cm^{-1} can be assigned to Co–O stretching mode [17].

The Raman spectra of the Co/MgO samples display a broad signal with maximum around 580 cm^{-1} (Fig. 3(d–f) and h*)* coincident with that seen in the spectrum of the solid solution. The shoulder at 665 cm^{-1} associated with Co_3O_4 is not observed. These results suggest that cobalt in these catalysts forms part of the solid solution, where Co^{2+} ions are located at octahedral position, substituting the Mg^{2+} sites in MgO lattice.

3.3. Surface characterisation

CO adsorption studies were performed on oxidised and reduced forms of Co(9 wt.%)/MgO, the catalyst showing the highest activity towards methane combustion, and comparisons made with Co(*x*)/MgO ($x = 3$, 6 and 12 wt.%) in reduced form, as well as the unpromoted MgO support.

3.3.1. MgO

For reference, studies of CO adsorption on pure MgO calcined at 1070 K were performed. An intense band is observed (spectrum not included), which gradually shifts from 2149 cm^{-1} for low coverage (0.5 h Pa) to 2147 cm^{-1} for high coverage (100 h Pa). This band is associated with pentacoordinated Mg ions on a [1 0 0] face, Mg^{2+}_{5cus}[18,19]. A shoulder at 2165 cm^{-1} is also present which shifts to lower frequencies as CO coverage increases. This band is due to coordinatively unsaturated (cus) Mg^{2+}_{4cus} located on edge and step sites [15,19].

IR spectra of CO adsorption at different temperatures reveal that the amount of adsorbed CO decreases as the temperature increases, causing the main band assigned to Mg^{2+}_{5cus}(2147 cm^{-1}) to lose intensity as surface CO coverage decreases. The shoulder at 2165 cm^{-1} associated with highly coordinatively unsaturated Mg^{2+} is still observed, but no bands related to carbonate or carboxylate species are observed.

3.3.2. Oxidised Co(9 wt.%)/MgO

Fig. 4 shows the IR spectra of CO adsorption at 85 K on Co(9 wt.%)/MgO. At low CO pressure (<0.3 hPa) a band envelope comprising two overlapping bands with maximum at 2160 cm^{-1} and two weak bands at 2114 and 2075 cm^{-1} are visible. As CO pressure increases, the two overlapping bands increase in intensity at what appears relatively the same rate, until at pressures greater than 5 hPa CO they can be resolved into a band at 2148 cm^{-1} and a shoulder at 2157 cm^{-1}. The very weak band at 2075 cm^{-1} is rapidly saturated upon admission of 0.3 hPa CO, whereas the band at 2114 cm^{-1} appears to decrease in intensity with added CO, until upon admission of 1 hPa it finally disappears. The bands observed on admission of CO at 85 K on this sample are summarised in Table 1.

The evolution of adsorbed carbonyl species with temperature (85–300 K) under a pressure of 100 hPa CO is shown in Fig. 5. The intensity of the main band envelope (2160 cm^{-1}) decreases as the temperature increases to 300 K. The band at 2114 cm^{-1}, on the other hand, reappears as the temperature reaches 120 K and increases in intensity as the surface coverage decreases. However, this too, disappears at near

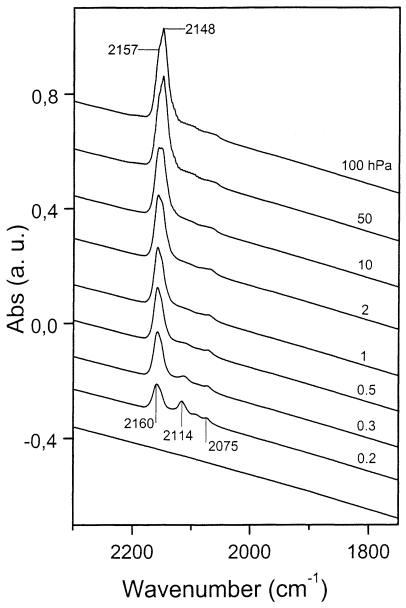

Fig. 4. IR spectra of CO adsorption on Co(9 wt.%)/MgO at 85 K. The bottom spectrum corresponds to the catalyst before any CO adsorption.

Table 1
Wavenumbers of CO adsorbed at 85 K on different sites in Co(*x*)/MgO

CO pressure (hPa)	MgO	9 wt.% Oxidation and reduction (670 K)[a]	9 wt.% Reduction (870 K)[a]	12 wt.% Reduction (870 K)[a]	6 wt.% Reduction (870 K)[a]	Sites
$P_{CO} < 1.5$	2149 (s)	2151 (sh)	2151 (sh)	2151 (sh)	2151 (sh)	Mg^{2+}_{5cus}
$P_{CO} > 10$	2147 (s)	2148 (s)	2148 (s)	2148 (s)	2148 (s)	
$P_{CO} < 1.5$		2160 (s)	2160 (s)	2160 (s)	2160 (s)	Co^{2+}_{5cus} and/or
$P_{CO} > 10$		2157 (sh)	2157 (sh)	2157 (sh)	2157 (sh)	Co^{2+}–O^{2-}
$0.1 < P_{CO} < 100$	2165 (sh)					Mg^{2+}_{4cus}
$P_{CO} < 1$		2114 (m)	2114 (m)	2114 (m)	2114 (m)	Mg^{2+} and/or Co^{2+} on steps
$0.1 < P_{CO} < 100$			2063 (w)	2063 (w)		Co^0

[a] Before the CO adsorption the catalyst was reduced in H_2 at the temperature indicated.

200 K. At temperatures of 150 K and above, a new series of bands at lower frequency becomes prominent (1705, 1680, 1396, 1295, 1274 and 1217 cm^{-1}). These bands have been assigned to oxidation products of CO in the form of carbonate-like surface species [20], which are absent on sintered MgO (see Table 2). These oxidised species may arise from the reduction of cobalt oxo-species (e.g. Co^{2+}–O^{2-})present on the surface.

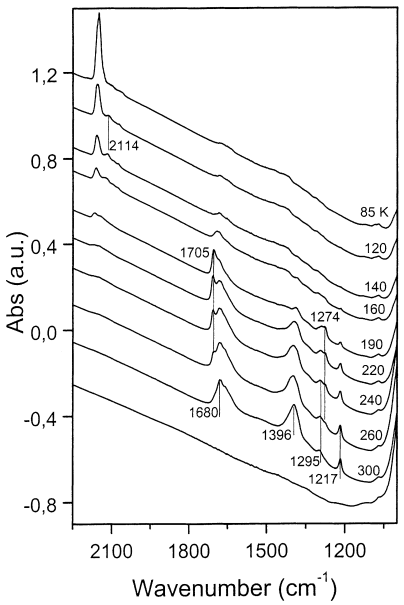

Fig. 5. IR spectra of CO adsorption on Co(9 wt.%)/MgO at different temperatures and 100 hPa CO. The bottom spectrum corresponds to the catalyst before any CO adsorption.

3.3.3. Reduced Co(9 wt.%)/MgO

After calcination at 870 K, the Co(9 wt.%)/MgO sample was reduced (under H_2 flow) at 670 K, and subsequently at 870 K. No significant changes were observed on adsorption of CO at 85 K after reduction of the sample at 670 K (see Table 1).

The spectra of CO adsorption at 85 K on Co(9 wt.%)/MgO reduced at 870 K are presented in Fig. 6. These results are comparable with those of the calcined sample except for a new band at 2063 cm^{-1}. The frequency of this band is characteristic of CO attached to Co^0 [21]. This signal saturates at low pressure and remains unchanged with increasing CO pressures (see Fig. 6). This suggests the presence of relatively few Co metal sites, most likely stemming from clustered surface Co^{2+} centres (with CoO-like behaviour) that can be easily reduced at 870 K. Note that the band at 2075 cm^{-1} seen in the oxidised sample is not observed.

The CO band in the region 2160–2147 cm^{-1} can now clearly be seen as resulting from the overlap of two bands at 2160 and 2151 cm^{-1} (for CO pressures lower than 1.5 hPa). The increase in CO coverage leads to a gradual shift to lower frequency for both bands, and saturation of the band at 2157 cm^{-1} at 2 hPa CO, but increased intensity of that at 2148 cm^{-1} (as shown in Fig. 7). These results suggest that the bands correspond to CO adsorbed on two different sites, which are tentatively assigned to Co^{2+} ions (2160 cm^{-1}) and cus Mg^{2+} (2151 cm^{-1}) LAS, both with octahedral coordination. The band at 2114 cm^{-1} is only observed at low coverage (<1 hPa CO) as seen in Fig. 6. It is attributed to abridging CO species bonded via both C and O ends to cus cationic sites present in steps, as pre-

Table 2
Wavenumbers of CO adsorbed at different temperatures on Co(*x*)/MgO

Temperature (K)	MgO	9 wt.% Oxidation and reduction (670 K)[a]	9 wt.% Reduction (870 K)[a]	12 wt.% Reduction (870 K)[a]	6 wt.% Reduction (870 K)[a]	Sites
85	2147 (s)	2148 (s)	2148 (s)	2148 (s)	2148 (s))	Mg^{2+}_{5cus}
$120 < T < 190$	2148	2152 (sh)	2152 (sh)	2152 (sh)	2152 (sh	
85		2157 (sh)	2157 (sh)	2156 (sh)	2157 (sh)	Co^{2+}_{5cus} and/or
$120 < T < 190$		2160	2160	2160	2160	Co^{2+}–O^{2-}
$120 < T < 220$		2114	2114	2114	2114	Co^{2+} on steps
$85 < T < 200$			2063	2063		Co^0
$T > 150$		1705[b], 1680, 1396, 1295, 1274[b], 1217	1705[b], 1682, 1396, 1276[b], 1217	1705[b], 1682, 1396, 1276[b], 1216	1705[b], 1680, 1396, 1295, 1274[b], 1217	Carbonates
$T > 200$			2090, 2063	2090, 2063		$Co^{2+}(CO)_3$
$T > 200$			1970, 1943	1970, 1943		$Co_y(CO)_x^-$
$T > 200$			2033, 1932, 1874, 1822	2033, 1932, 1874, 1822		$Co(CO)_4^-$

[a] Before the CO adsorption the catalyst was reduced in H_2 at the temperature indicated.
[b] Those bands are strong at 160 K and shoulder at 300 K.

viously found in KCl films [22]. This species probably changes to end-on configuration (terminal carbonyl), as the CO pressure increases. The fact that this species is not observed in the pure support material, suggests that bonding from at least one end must be to a Co site.

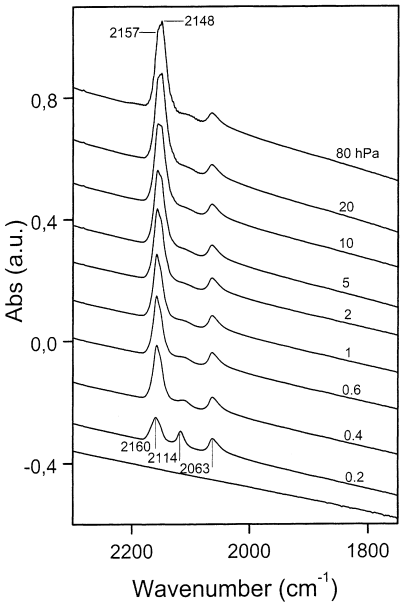

Fig. 6. IR spectra of CO adsorption at 85 K on Co(9 wt.%)/MgO reduced at 870 K in H_2. The bottom spectrum corresponds to the catalyst before any CO adsorption.

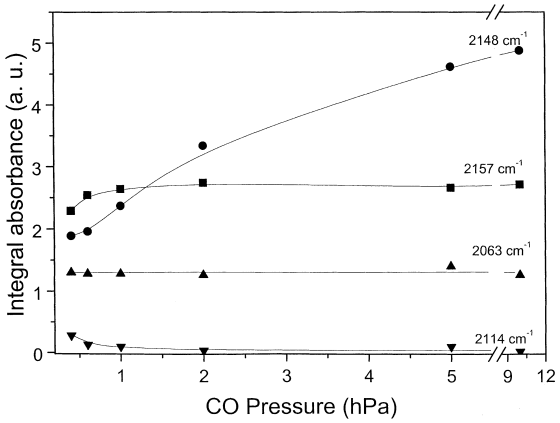

Fig. 7. Integral intensities of CO bands on Co(9 wt.%)/MgO reduced at 870 K in H_2 for different CO pressures at 85 K.

The evolution of adsorbed CO on reduced Co(9 wt.%)/MgO as the temperature is raised from 110 to 300 K under a CO pressure of 80 hPa is shown in Fig. 8. The disappearance of carbonyl species and the subsequent development of carbonate species on this solid follow the same pattern as seen in the oxidised sample. However, a new series of bands appear in the 2100–1750 cm^{-1} region at 210 K. These bands, at 2090, 2063, 2033, 1970, 1943, 1932, 1874 and 1822 cm^{-1}, can be assigned to Co carbonyl complexes [13,14,21–24]. Rao et al. [21] found that nucleophilic attack by surface O^{2-} on CO adsorbed on metal

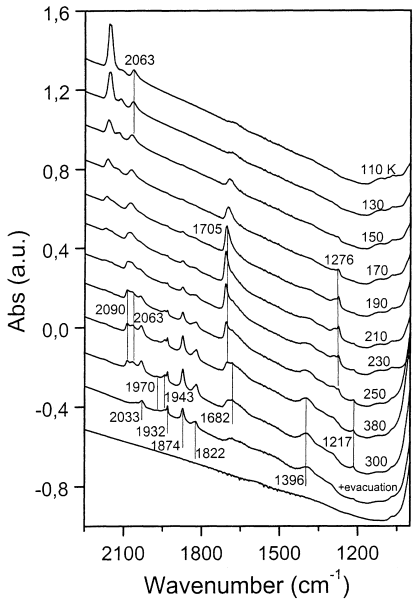

Fig. 8. IR spectra of CO adsorption at different temperatures and 80 hPa CO on Co(9 wt.%)/MgO reduced at 870 K in H_2. The bottom spectrum corresponds to the catalyst before any CO adsorption.

cobalt particles supported on MgO, leads to the formation of $Co(CO)_4^-$ and CO_3^{2-}. The free $Co(CO)_4^-$ belongs to T_d symmetry group and has only one IR peak. However, when $Co(CO)_4^-$ interacts with the surface, changes in its symmetry are expected. Rao et al. [21] proved that the new local symmetry is C_{2v}, having four IR bands. Thus, the bands at 2033, 1932, 1874 and 1822 cm^{-1} are assigned to $Co(CO)_4^-$ (see Table 2).

The four bands associated with $Co(CO)_4^-$ and a further two at 1970 and 1943 cm^{-1} remain after evacuation at room temperature (Fig. 8). The two shoulders at 1970 and 1943 cm^{-1} could be due to the formation of some clustered anionic complexes, $Co_y(CO)_x^-$ [21]. These Co carbonyl complexes are deemed to be irreversibly bonded to the surface at room temperature, as was reported by Zecchina et al. [13]. On the other hand, the bands at 2090 and 2063 cm^{-1} disappeared after evacuation at room temperature, thus are likely to belong to another Co complex, such as $Co^{2+}(CO)_3$. According to Zecchina et al. [13] the spectra of $Co^{2+}(CO)_3$ on a MgO–CoO solid solution consists of two peaks in the 2100–2040 cm^{-1} range.

3.3.4. Reduced Co(12 wt.%)/MgO

The main features of CO adsorption on reduced Co(12 wt.%)/MgO are summarised in Tables 1 and 2. Even though the Co content is increased in this sample, the spectra (not shown) display the same bands and relative intensity ratios as those of Co(9 wt.%)/MgO. This suggests that the surface species and their concentrations are quite similar in the two samples. These results are in agreement with their catalytic activities, the kinetic rate of methane combustion over Co(12 wt.%)/MgO being almost the same as that measured over Co(9 wt.%)/MgO (Fig. 1).

3.3.5. Co(6 wt.%)/MgO and Co(3 wt.%)/MgO

Even though Co(6 wt.%)/MgO was reduced at 870 K, the spectra of CO adsorption at 85 K (and the ensuing evolution of adsorbed species with temperature) showed the same adsorbed species as present in calcined, but not reduced, Co(9 wt.%)/MgO (see Tables 1 and 2). The absence of the band at 2063 cm^{-1}, characteristic of CO attached to Co^0, suggests that the surface Co^{2+} is well dispersed, and that any clustered Co^{2+} formed is not large enough to behave as bulk cobalt oxide, which is easily reducible at 870 K. This is further supported by the fact that on elevation of the temperature in the presence of CO (100 hPa), carbonates are formed as in the calcined 9 wt.%

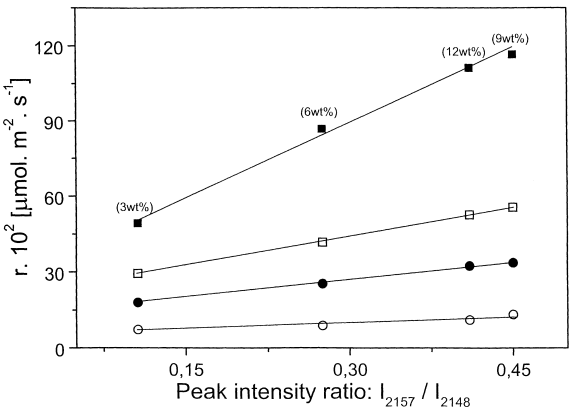

Fig. 9. Correlation between kinetic rate of reaction over Co(x)/MgO (x = 3, 6, 9 and 12 wt.%) at different reaction temperature and the integral absorbance ratios of the 2157 and 2148 cm^{-1} bands (I_{2157}/I_{2148}). Reaction conditions: CH_4 2 vol.%; O_2 8 vol.%; N_2 balance, and space velocity: 480,000 h^{-1}. Symbols: (○) 820 K, (●) 845 K, (□) 870 K, (■) 895 K.

sample, but not carbonyl complexes appeared as in the reduced 9 and 12 wt.% samples.

The adsorbed CO species on Co(3 wt.%)/MgO are the same as Co(6 wt.%)/MgO. However, the ratios of the integral intensities of bands at 2157 and 2148 cm^{-1} after saturation (I_{2157}/I_{2148}) do vary for the two samples, indicating a difference in the amount of surface Co present. Indeed, this ratio increases with the Co loading throughout the range of samples (Fig. 9). In the case of Co(12 wt.%)/MgO, however, the ratio is quite similar to that for Co(9 wt.%)/MgO.

4. Discussion

4.1. Solid solution formation

The Co/MgO catalysts calcined at 1070 K have been shown to be active towards high temperature methane combustion (Fig. 1). Seeing as the MgO support alone is inactive for this process under the conditions studied, it would appear that Co (in some form) serves as the active surface site. The catalytic activity (as depicted by the reaction rate at each of the four temperatures) increases with cobalt loading, but reaches a plateau at ca. 9 wt.% Co content (Fig. 1). This could be explained by assuming that Co is present in dispersed form up to that point, and that at higher loadings, agglomeration of Co to form an oxide phase (e.g. Co_3O_4) takes place, thus, reducing the available Co surface area and so limiting the catalytic activity observed. However, no sign of the Co_3O_4 spinel was detected by XRD in any of the samples, though this could be explained by small crystallite size. Examination of the results from TPR measurements and Raman spectroscopy also confirms the absence of this oxide phase. Moreover, the data obtained from these three techniques indicate that cobalt forms a solid solution with MgO, which is present at all Co loadings.

CoO and MgO are known to form solid solutions in which Co^{2+} ions are located at octahedral positions, substituting Mg^{2+} sites in the MgO lattice [7–9]. This solid solution maintains the structure of MgO, a NaCl-type crystal structure, where the [1 0 0] face is preferentially exposed. Surface ions of Mg^{2+} and isolated Co^{2+} are reported to be located on (i): [1 0 0] faces, and (ii): edges, steps, corners and kinks [12,13], though it should be kept in mind that, as the samples are sintered, crystallite dimensions increase, decreasing the fraction of surface ions located at edges, steps, corners and kinks, preferentially exposing the [1 0 0] faces. In concentrated solid solution (ca. 30 wt.%), however, clustered Co^{2+} can also be present on the surface [14], which, when attaining a certain number of bulk Co^{2+} ions, can show oxide-like (CoO) behaviour.

4.2. Distribution of surface Co sites

Seeing as the CoO–MgO solid solution present in each of the Co/MgO samples studied is a bulk phase, it seems unlikely that its presence can solely account for the variation in activity shown by the different samples. Hence, the question of how the Co^{2+} ions are ordered on the surface of the Co(x)/MgO catalysts become all important. The characterisation of the Co/MgO surfaces is now discussed in terms of the assignments for each vibrational band observed (Tables 1 and 2).

4.2.1. CO adsorption: bands at 2160–2147 cm^{-1}

In sintered MgO, the band at 2149 cm^{-1} which shifts to 2147 cm^{-1} as CO pressure increases, is associated with pentacoordinated Mg^{2+} ions (Mg^{2+}_{5cus}) on the exposed [1 0 0] face [18,19]. The adsorbed CO is in end-on configuration, bonded to the Mg^{2+} cationic site through a σ-bond with the C atom. A shoulder at 2165 cm^{-1} is due to coordinately unsaturated Mg^{2+}_{5cus} sites located on edges and steps [15,19]. Consequently, the bands shifting from 2151 to 2148 cm^{-1} observed in the IR spectra of all Co/MgO samples are assigned to large patches of pentacoordinated Mg^{2+} ions on [1 0 0] faces.

In the Co/MgO samples the band around 2160 cm^{-1} is most likely associated with CO adsorbed on cus Co^{2+} surface sites. Kadinov et al. [25] proposed that the band around 2160 cm^{-1} for adsorbed CO on Co/Al_2O_3 corresponds to CO^+ on highly coordinatively unsaturated Co^{2+}_{3cus}. This assignment is incorrect for Co(9 wt.%)/MgO, since this would mean that most of the Co^{2+} on these low surface area samples ware located on the most exposed positions (corners and kinks), which are comparatively few. Little suggested in his book [26] that bands around 2200–2140 cm^{-1} were associated with CO adsorbed on transition metal oxo-species, where the metal–oxygen bond is weak.

The surface O^{2-} species on CoO–MgO has previously been reported by Cordischi et al. [27], and appears to be favoured by increasing cobalt content. It is also quite stable, needing a high evacuation temperature of 1173 K to be removed. In the same vein, the results obtained by Cimino and Pepe [28] show that Co^{2+} plays a significant role in the formation of O^{2-} species. Thus, a possible assignment for the signal around 2160 cm^{-1}, which is still present in samples reduced at 870 K, is CO adsorbed on Co^{2+} within an oxo-species, e.g. surface Co^{2+}–O^{2-}. Alternatively, adsorption could be occurring on cus Co^{2+} sites (five-coordinate) which are part of a CoO–MgO solid solution.

4.2.2. CO adsorption: band at 2114 cm^{-1}

This band is assigned to CO bonded through both C and O ends at cus cation sites on steps, as was found on KCl film [22], the crystallites of which have the same crystal structure as MgO and the CoO–MgO solid solution. The interaction of CO with cations via the oxygen lone pairs lowers its stretching frequency [22]. This band is only observed at very low coverage where the limited number of CO molecules are attracted by a greater number of cus cationic LAS. This species probably changes to end-on configuration (i.e. terminal carbonyl through the C atom) as the CO pressure increases, thus, disappearing from the spectra. This band is not present in spectra taken of the MgO support alone (Tables 1 and 2), which suggests that an exposed Co^{2+} cation (Co^{2+}_{4cus}) is required at a step site for such bridging species to form.

4.2.3. CO adsorption: band at 2075 cm^{-1}

According to Zecchina et al. [19], this band can be assigned to a stretching vibration of ketenic C=C=O groups (2120–2070 cm^{-1}) from $C_nO_{n+1}{}^{2-}$ species formed by interaction of CO with unsaturated O^{2-}_{3cus} ions located on corners. They are presumably formed by a process similar to the following reaction [30]:

$$3CO + 2O^{2-}_{cus} \rightarrow C_2O_2{}^{2-} + CO_3{}^{2-} \quad (1)$$

4.2.4. CO adsorption: band at 2063 cm^{-1}

This band is present only on high Co loading samples (9 and 12 wt.% Co) reduced at 870 K (Table 1). Its frequency is characteristic of CO bound to Co^0 [21]. Fig. 6 shows how this signal on Co(9 wt.%)/MgO reduced at 870 K saturates at low CO pressure (0.2 hPa) and remains unchanged with the increase of CO coverage, which indicates the presence of relatively few sites. Note that, neither of the two samples displays a band at 2075 cm^{-1}, suggesting that clustered Co^{2+} ions are involved in the formation of Co metal particles. The properties of the clustered Co^{2+} ions might resemble those of bulk CoO, which is easier to reduce with H_2 at high temperature than isolated Co^{2+} ions or MgO [14]. Therefore, the 2063 cm^{-1} band is assigned to CO interacting with small particles of Co^0, created through reduction of small Co^{2+} clusters.

4.2.5. CO adsorption: bands between 1705–1217 cm^{-1}

The generation of various carbonate species with increasing temperature is observed for all samples except calcined MgO (Table 2). These species are most likely the result of CO oxidation at Co surface sites, followed by readsorption of the generated CO_2 on the basic O^{2-} sites of MgO. The presence of oxo-species on the surface of Co-containing solids, which are capable of acting as an oxygen reservoir for this process, has already been reported in the literature [28,29]. The bands at 1705, 1274 and 1217 cm^{-1} are assigned to a bridged organic-like carbonate species (1774–1710, 1270–1220 cm^{-1} [30]); the bands at 1680 and 1295 cm^{-1} to bidentate carbonate (1670 and 1307 cm^{-1} [31]); and cm^{-1} for the band at 1396 cm^{-1} to a monodentate carbonate (cf. 1408 cm^{-1} for Co_3O_4 [32]; 1390MgO [31]).

4.2.6. CO adsorption: bands between 2090–1822 cm^{-1}

The bands at 2090, 2063, 1970, 1943, 2033, 1932, 1874 and 1822 cm^{-1} are present on reduced, high Co loading (9 and 12 wt.%) samples at temperatures above 150 K, and are stable at ambient temperature even under vacuum. The bands are not present in any other sample.

The presence of a $Co^{2+}(CO)_3$ complex is inferred due to the two bands at 2090 and 2063 cm^{-1}. Zecchina et al. [13] maintain that the interaction between Co^{2+} ions on edges of CoO–MgO and gas phase CO give rise to $Co^{2+}(CO)_3$ and $[COCo(CO_2)_2]^{2-}$ species at room temperature. In our samples, no bands related to $[COCo(CO_2)_2]^{2-}$ are detected, and the presence of $Co^{2+}(CO)_3$ is only observed on reduced solids

with high Co loadings (Table 2). Presumably, the Lewis base assisted redox disproportionation of two or more mononuclear Co^0 carbonyl leads to the ionic species, $Co^{2+}(CO)_3$ and $Co(CO)_4^-$ [33]. The four bands at 2033, 1932, 1874 and 1822 cm^{-1} are associated with $Co(CO)_4^-$ [21,23], the formation of which could also be brought about through nucleophilic attack of the basic surface O^{2-} ions on CO adsorbed on Co^0, according to the following reaction [21]:

$$2Co^0(CO) + 2O^{2-} + 3CO_{(g)} \rightarrow 2Co(CO)_4^- + CO_3^{2-} \quad (2)$$

The two shoulders at 1970 and 1943 cm^{-1} are reportedly due to the formation of some clustered anionic complexes, $Co_y(CO)_x^-$ [21].

In all cases, Co^0 clusters are necessary for the formation of these Co carbonyl complexes. In other words, the presence of the carbonyl complexes is evidence of clustered Co on the surface of reduced 9 and 12 wt.% Co/MgO.

4.2.7. Summary of CO adsorption on Co(x)/MgO (x = 3, 6, 9 and 12 wt.%)

The adsorption of CO at 85 K and the evolution of adsorbed species with temperature on the range of Co/MgO samples, can be summarised by the following statements:

1. Patches of Mg^{2+}_{5cus} as well as Co^{2+} oxo-species and/or Co^{2+}_{5cus} are present on the surface of all the Co/MgO samples. The Co species are possibly situated on the exposed sites within a CoO–MgO solid solution.
2. At low CO coverage, CO forms a bridging species on cationic sites in steps, which are not seen on MgO. These species revert to the terminal monocarbonyl at higher coverage.
3. Clustered Co^0 (metal) is only detected on high Co loading (9 and 12 wt.%) catalysts after reduction at 870 K. Saturation occurs at low CO pressure indicating the presence of relatively few surface sites.
4. Carbonates are formed at temperatures above 150 K on all Co-containing samples. These species are most likely the result of CO oxidation at Co surface sites, followed by readsorption of the generated CO_2 on the basic O^{2-} sites of MgO.
5. Carbonyl complexes are formed only above 210 K in the two samples (9 and 12 wt.%, reduced 870 K) displaying clustered Co^0.
6. Surface Co concentrations and distributions on Co (9 wt.%)/MgO and Co (12 wt.%)/MgO are almost the same.

4.3. Relationship between catalytic activity and distribution of Co sites

What remains to be established is the link between the surface distribution of Co throughout the range of Co/MgO samples and their activity towards methane combustion. It is clear that activity increases with Co content up to 9 wt.% Co at all four temperatures studied (Fig. 1). It is also apparent that further addition up to 12 wt.% Co, has no further influence upon the activity. Characterisation of the bulk has established that these features are not due to the presence of a Co_3O_4 phase. Indeed, instead of a separate oxide phase, Co is incorporated into the MgO lattice and forms a solid solution of CoO–MgO at all loadings.

To elucidate why the 9 and 12 wt.% Co-containing solids have almost the same surface properties and activity requires examination of the preparation method. Addition of $Co(NO_3)_2$ solution to the MgO slurry in water (pH = 12) causes precipitation of $Co(OH)_2$ because of the high pH value. Consequently, an equal amount of Mg^{2+} is dissolved to compensate for the NO_3^- anions released. On evaporation of water, precipitation of the Mg salt occurs which covers part of the freshly deposited $Co(OH)_2$. During the ensuing calcination process at high temperatures, the former becomes MgO, whilst the latter is incorporated into a bulk CoO–MgO solid solution. This results in patches of MgO on the catalyst surface leading to a non-homogeneous surface Co distribution. Hence, the presence of MgO islands strongly affects the properties of the high loading Co/MgO catalysts by obscuring the active Co sites.

This can be seen in Fig. 9, which shows a linear correlation between initial rate of reaction for methane combustion and the ratio of integral band intensities, I_{2157}/I_{2148}. This ratio is taken from calculating the intensities of bands at 2157 and 2148 cm^{-1} on saturation with CO; the former being attributed to cus Co^{2+} sites and the latter to surface Mg^{2+} in MgO islands. It can be seen that I_{2157}/I_{2148} increases between the

lower Co loading samples, but actually decreases between 9 and 12 wt.%, which supports the theory that the amount of exposed Co^{2+} is not directly samples and the proportion of exposed Co^{2+} is attainable from the proportional to the increase in Co loading. However, a direct relationship between the activity of the Co/MgO graph.

What can be suggested, therefore, is that at low loadings only a small proportion of the Co going into the solid solution is present on exposed faces. However, as the Co content of the samples increases, a larger amount is exposed on the surface. These Co^{2+} sites are accessible in comparison to those held in the bulk, and hence, activity increases with surface Co^{2+} content. This effect is seen up to 9 wt.% Co, after which the increase in exposed Co^{2+} sites is encountered by the masking effect of the islands of MgO.

However, Co is not fully incorporated into the solid solution at high Co loadings and forms small clusters, which shows bulk CoO-like behaviour in that they are readily reduced at 870 K. This is evidenced by the presence of Co metal clusters in the 9 and 12 wt.% samples after reduction at 870 K. Hence, the benefit of having surface Co^{2+} species is balanced by the clustering effect of these species, which leads to their easy reduction, negating their contribution to the overall catalytic activity of the samples.

5. Conclusions

At all Co contents a CoO–MgO solid solution is formed. No separate Co_3O_4 phase is detected, though in samples with high loading (9 and 12 wt.% Co) Co^{2+} clusters are found whose behaviour mimics that of bulk CoO. On reduction at 870 K these sites form Co^0 clusters, which induce complex carbonyl formation at temperatures above 210 K. However, the degree of surface exposure in these Co^{2+} clusters is small and hence, they are deemed to have little influence on the catalytic activity. This was found to be proportional to the fraction of Co^{2+} on exposed faces, either as Co^{2+} oxo-species or Co^{2+}_{5cus}, within the CoO–MgO solid solution. Loading above 9 wt.% Co produced no further benefit due to the formation of MgO islands which blocked the active Co sites. MgO can be deemed to be a good support for Co, capable of maintaining dispersed Co^{2+} sites even after reduction at 870 K.

Acknowledgements

The work done in Munich was financially supported by the Deutsche Forschungsgemeinschaft (SFB 338) and the Fonds der Chemischen Industrie. MAU, RS and EL wish to acknowledge the financial support received from CONICET, ANPCyT and UNL (CAI+D'96). Thanks are also given to the Japan International Cooperation Agency (JICA) for the donation of Raman, XRD and TPR equipments. MAU acknowledges the financial aid provided by FOMEC 824 (UNL) for her stay in Munich.

References

[1] H. Arai, M. Machida, Catal. Today 10 (1991) 81.
[2] J.G. Mc Carty, H. Wise, Catal. Today 8 (1990) 231.
[3] D.L. Trimm, Catal. Today 26 (1995) 231.
[4] M. Berg, S. Järås, in: H. Arai (Ed.), Proceeding of the International Workshop on Catalytic Combustion, Tokyo, Japan, 18–20 April 1994, p. 32.
[5] M. Berg, S. Järås, Appl. Catal. A.: General 114 (1994) 227.
[6] E. Giamello, E. Garrone, S. Coluccia, G. Spoto, A. Zecchina, in: G. Centi, F. Trifiró (Eds.), New Developments in Selective Oxidation, Elsevier, Amsterdam, 1990, p. 817.
[7] A. Hagan, M. Lofthouse, F. Stone, M. Trevethan in: B. Delmon, P. Grange, P. Jacob, G. Poncelet (Eds.), Scientific Bases for the Preparation of Heterogeneous Catalysts, Elsevier, Amsterdam, 1979, p. 417.
[8] A. Cimino, F.S. Stone, in: G. Ertl, H. Knözinger, J. Weitkamp (Eds.), Handbook of Heterogeneous Catalysis, Vol. 2, Wiley-VCH, Weinheim, 1997, p. 845.
[9] H. Asakura, Y. Iwasawa, Mater. Chem. Phys. 18 (1988) 499.
[10] H. Knözinger, in: G. Ertl, H. Knözinger, J. Weitkamp (Eds.), Handbook of Heterogeneous Catalysis, Vol. 2, Wiley-VCH, Weinheim, 1997, p.707.
[11] H. Knözinger, in: E. Umbach, H.J. Freund (Eds.), Adsorption on Ordered Surfaces of Ionic Solids and Thin Films, Springer, Berlin, 1993.
[12] A. Zecchina, G. Spoto, S. Coluccia, E. Guglieminotti, J. Phys. Chem. 88 (1984) 2575.
[13] A. Zecchina, G. Spoto, E. Borello, E. Giamello, J. Phys. Chem. 88 (1984) 2582.
[14] A. Zecchina, G. Spoto, E. Garrone, A. Bossi, J. Phys. Chem. 88 (1984) 2587.
[15] D. Scarano, G. Spoto, S. Bordiga, S. Coluccia, A. Zecchina, J. Chem. Soc., Faraday Trans. 88 (3) (1992) 291.
[16] H. Ohtsuka, T. Tabata, O. Okada, L.M.F. Sabatino, G. Bellussi, Catal. Lett. 44 (1997) 265.
[17] H. Ohtsuka, T. Tabata, O. Okada, L.M.F. Sabatino, G. Bellussi, Catal. Today. 42 (1998) 45.
[18] M. Zaki, H. Knözinger, Spectrochim. Acta 43A (1987) 1459.
[19] A. Zecchina, S. Coluccia, G. Spoto, D. Scarano, L. Marchese, J. Chem. Soc., Faraday Trans. 84 (1990) 703.
[20] G. Busca, V. Lorenzelli, Mater. Chem. 7 (1982) 89.

[21] K.M. Rao, G. Spoto, A. Zecchina, J. Catal. 113 (1988) 466.
[22] D. Scarano, A. Zecchina, J. Chem. Soc., Faraday Trans. I 82 (1986) 3611.
[23] K.M. Rao, G. Spoto, E. Guglielminotti, A. Zecchina, J. Chem. Soc., Faraday Trans. I 84 (1988) 2195.
[24] M. Kurhinen, T. Pakkanen, Langmuir 14 (1998) 6907.
[25] G. Kadinov, Ch. Bonev, S. Todorova, A. Palazov, J. Chem. Soc., Faraday Trans. 94 (1998) 3027.
[26] H. Little, Infrared Spectra of Adsorbed Species, Academic Press, London, 1966, p. 67.
[27] D. Cordischi, V. Indovina, M. Occhiuzzi, A. Arieti, J. Chem. Soc., Faraday Trans. I 75 (1975) 533.
[28] A. Cimino, F. Pepe, J. Catal. 25 (1972) 362.
[29] D. Gazzolli, M. Occhiuzzi, A. Cimino, D. Cordischi, G. Minelli, F. Pinzari, J. Chem. Soc., Faraday Trans. I 92 (1996) 4567.
[30] E. Guglielminotti, S. luccia, E. Garrone, L. Cerruti, A. Zecchina, J. Chem. Soc., Faraday Trans. I 75 (1979) 96.
[31] R.S.C. Smart, T.L. Slager, L.H. Little, R.G. Greenler, J. Phys. Chem. 77 (1973) 1019.
[32] A.J. Goodsel, J. Catal. 30 (1973) 175.
[33] A. Zecchina, C. Otero Orean, Catal. Rev.-Sci. Eng. 35 (1993) 261.